

Time profile of temperature rise in assemblies of nanomagnets

J.-L. Déjardin and H. Kachkachi*

*Université de Perpignan via Domitia, Lab. PROMES CNRS UPR8521,
Rambla de la Thermodynamique, Tecnosud, 66100 Perpignan, France*

(Dated: May 30, 2022)

We compute the heat generated by (non-interacting) nanomagnets subjected to an alternating magnetic field (AMF) and study its transfer to the hosting medium and environment. For the first task, we compute the heat generated by the nanomagnets (or the specific absorption rate \mathfrak{S}) using the ac susceptibility in the linear regime. For the second task, the loss of heat to the environment is modeled with the help of a balance (macroscopic) equation based on Newton's law of cooling. This equation is solved both numerically and analytically for a generic ferrofluid and the analytical solution renders a very good approximation to the general balance equation. Then, we investigate the effects of AMF frequency and amplitude on the temperature elevation during its temporal evolution. Finally, using the available experimental data for maghemite and magnetite ferrofluids, we discuss the behavior of Newton's heat transfer coefficient in terms of the AMF amplitude and frequency. These results could trigger experimental investigations of this coefficient which characterizes the rate of heating in a ferrofluid, with the aim to build more refined models for the mechanisms of heat generation and its diffusion in ferrofluids used in magnetic hyperthermia.

PACS numbers:

I. INTRODUCTION

The process of magnetic hyperthermia (MH) occurring in assemblies of magnetic nanoparticles, or nanomagnets (NM), offers a significant advantage over the traditional methods for cancer treatment [1–5] based on the necrosis of the cancerous cells by irradiation [6], as it avoids the side effects of the latter by a directed and localized heating. Moreover, MH has been shown to kill cells faster than the traditional methods and this reduces the therapy administration time [7]. However, at the present time the mechanism by which the heat is generated and diffused in the assembly of NM is not fully understood.

In MH, the NM are heated with the help of an external AC magnetic field, that is a time-dependent (alternating) magnetic field (AMF), and the optimization of the whole process depends on several factors, such as the magnetic field itself (amplitude and frequency), NM size and concentration, and solution viscosity [8–12]. The efficiency of MH may be assessed through the *specific absorption rate* (SAR), usually given in Watt per gram (W/g). The SAR has been investigated by many research groups by computing the area of the hysteresis loop of the magnetization as a function of the AC field intensity, for a given frequency [8–11, 13, 14]. With the desire to obtain (approximate) analytical expressions, an alternative approach was adopted in Refs. [15–17] which exploits the fact that the system absorption of the electromagnetic energy brought in by the AMF may be described by the out-of-phase component of the dynamic response function, the AC susceptibility.

Another observable that is being actively used and

which is quite relevant for characterizing MH and assessing its efficiency is the temperature rise after the start of heating, upon varying the AMF characteristics and the sample's properties [18–20]. This technique is useful as it allows for a more precise control of the temperature rise in MH in order to reduce the risk of heating the surrounding healthy cells. A detailed discussion of this calorimetric method and its comparison with other methods is presented in Ref. [19]. Various empirical equations are used to model the temperature rise in MH and the initial slope of $T(t)$ is used for estimating the SAR on the ground of two assumptions: i) upon switching on the AMF, the sample temperature remains homogeneous, and ii) the heat losses are negligible at short times. However, this initial-slope technique has a few drawbacks exemplified, for instance, by the fact that it is based on a simplified model which ignores the heat diffusion across the sample and that the determination of the initial-time slope is performed at a transient state of the sample temperature [19, 21–23]. It also ignores the heat flow from the sample into its environment. It would then be desirable to go a step further and take into consideration both the heating of the sample via the excitation of NM by the AMF and the diffusion of the thus-generated heat into the sample and ultimately the heat loss toward the environment. However, the issue of heat flow in suspensions is rather involved and one has to proceed in steps to separately investigate each one of these mechanisms. Regarding the efficiency of heat flow in nanofluids and, in general heat transport at the nanoscale, there is a rich literature studying the underlying mechanisms with attempts to extend Fourier's law, see for instance Refs. [24–28].

In the present work, we study the balance between the heat generated by the NM subjected to the AMF and the heat lost to the sample's immediate environment, a balance that turns out to determine the temperature

*Electronic address: hamid.kachkachi@univ-perp.fr

time profile observed in ferrofluids. For this purpose, we present a phenomenological study of the heat exchange of a (non-interacting) polydisperse assembly of NM, subjected to an external AMF, with its environment. More precisely, we compute the heat Q generated by the nanomagnets (or the SAR \mathfrak{S}) through the dynamic response given by the out-of-phase component of the AC susceptibility (χ'') of the system. Next, we describe the loss of this heat to the environment with the help of a balance equation including a term that describes a kind of Newton's law of cooling. The latter involves a phenomenological coefficient L_n , the heat transfer coefficient, which we estimate for two NM species, the maghemite and magnetite, using the experimental data available for these materials and variable AMF characteristics (amplitude and frequency) [18, 20]. The coefficient L_n provides us with an additional means for assessing the rate of heat losses to the environment and the corresponding results obtained here, for various parameters of the NM assembly, could be checked in future experiments. This could then help to develop a more refined model for the mechanisms of heat generation and losses in NM assemblies used in MH.

We would like to add a final word regarding the comparison of our model with experiments. First of all, we emphasize that our objective here is not to build a model that would quantitatively fit the curves measured for polydisperse assemblies of nanomagnets. This would not be possible, anyway, given the various simplifications, exemplified by the absence of inter-particle interactions. Instead, the main idea to compare with experiments our results for the time profile of the temperature elevation is twofold:

1. Show that, at the time scales investigated in experiments, the observed temperature profile is mostly determined by the balance equation that accounts for i) the conversion into heat of the electromagnetic energy brought in by the AMF and ii) its loss into the environment.

2. Estimate the order of magnitude of the Newton coefficient and investigate its dependence on the AMF characteristics that are accessible to today's measurements.

II. MODEL FOR HEAT GENERATION AND LOSS

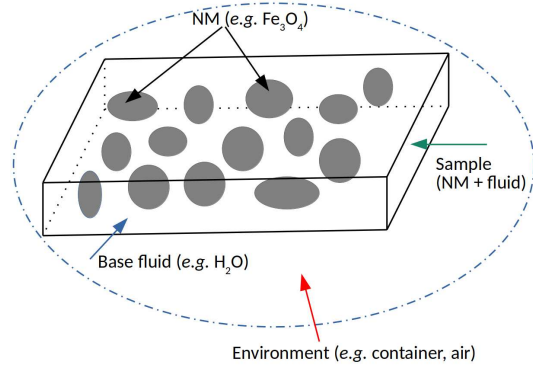


Figure 1: Sketch of the model system: a sample composed of nanomagnets (NM) as heat sources, and the embedding fluid (base fluid), coupled to its environment (air).

We start by defining the model system which we use for studying the diffusion mechanisms of the heat generated by the nanomagnets (NM) into their hosting medium and then to the environment. Our model system is sketched in Fig. 1. It is composed of

1. the sample (ferrofluid): an assembly of nanomagnets (magnetite, for instance) floating in a fluid, the base fluid (bf), which is chosen here to be water,
2. the environment: may be the container of the sample (a tube, a box) or air.

In the general scheme for SAR measurement, the sample is initially set to the same temperature as its environment, T_0 . Then, the AMF is switched on at $t = 0$. The latter excites the NM which then release heat within the sample, *i.e.* they heat up the fluid. The heat thus generated then diffuses across the sample and the heat flux reaches the sample's limits, or its interface with the environment, to which the heat is transferred by conduction, convection or radiation. If we assume that the NM are homogeneously distributed through the sample, the heat power by unit volume is $\mathfrak{S}/V_{\text{ff}}$, where V_{ff} is the volume of the whole sample (NM + base fluid), *i.e.* the ferrofluid.

A. Heat balance equation

The time evolution of the temperature within the sample, measured at position \mathbf{r} , is governed by the heat-diffusion equation with sources, namely [19]

$$\rho c_v \frac{\partial T}{\partial t}(\mathbf{r}, t) - \kappa \nabla^2 T(\mathbf{r}, t) = \mathcal{P}/V_s, \quad (1)$$

where ρ (kg/m^3), c_v ($\text{J}/\text{K}/\text{kg}$), and κ ($\text{W}/\text{K}/\text{m}$) are respectively the density, the specific heat and the thermal

conductivity of the sample, all assumed to be uniform. $\mathcal{P}(W)$ is the heat power and V_s the sample volume. In this case, Eq. (1) can be solved analytically, but in practice it is more efficient to make use of optimized numerical algorithms. For the calculation of the SAR, a simpler model may be derived if one ignores the temperature gradients within the sample, upon which the spatial derivative of T is dropped from the equation above. Obviously, this temperature gradient is what conveys the heat generated by the NM to the environment. Nevertheless, this assumption may apply if the (thermal) relaxation time within the sample is much shorter than the relaxation time of heat diffusion through the sample-environment interface. In practice, this may be achieved by using a highly conductive sample with a weak link to its environment. Within this approximation, one may derive the temporal evolution of the temperature within the sample from the power balance between the sample (NM + BF) and its environment. Accordingly, upon dropping the gradient term from Eq. (1) and adding the contribution of the heat flow (power loss) from the sample into the environment, we obtain the following balance equation (upon multiplying by the sample volume V_{ff})

$$C_{\text{ff}} \frac{dT}{dt} = \mathcal{P}(T) - L_{\text{ff}} [T(t) - T_0]. \quad (2)$$

Here $C_{\text{ff}} = \sum_i c_i m_i$ is the heat capacity (in J/K) of the sample. We have introduced the coefficient L_{ff} (W/K) as the analog of the heat transfer coefficient between the sample and its environment. This equation implies that the temperature rise in the ferrofluid is the result of a balance between the heat power generated by the NM (within the ferrofluid) and the heat power lost to the environment. The last process is described here by the so-called Newton's law of cooling [see the textbook [29] for a more general discussion]. At the initial time $t = 0$, when the AC field is switched on, we have $T(t = 0) = T_0$, which is the temperature of the sample. Note that $\mathcal{P}(T)$ in Eq. (2) is the total heat power generated by the entire assembly of NM. Hence, if one computes the SAR for a single NM, one has to multiply by the total number of NM in the ferrofluid.

In Ref. [19], C_{ff} , \mathcal{P} and L_{ff} were assumed to be constant upon which the equation above is analytically solved as follows

$$T(t) = T_0 + \Delta T_{\text{max}} \left(1 - e^{-t/\varsigma}\right) \quad (3)$$

where $\Delta T_{\text{max}} = \mathcal{P}/L_{\text{ff}}$ and $\varsigma = C_{\text{ff}}/L_{\text{ff}}$. Thus, in the steady state ($t \rightarrow \infty$), the heat generated and that lost become equal and the sample temperature remains constant at $T_{\text{max}} = T_0 + \Delta T_{\text{max}}$.

B. SAR from linear response

Next, we discuss the calculation of the SAR. This may be inferred either from the area of the dynamic hysteresis

loop or from the dynamic response of the system represented by the AC susceptibility. A detailed discussion can be found in Refs. [15–17] and references therein. In both cases, one is faced with a nonlinear problem which makes it rather difficult, if not impossible, to come up with an analytical solution. However, the general situation can be tackled with the help of a numerical algorithm that could proceed as follows: the Landau-Lifshitz-Langevin equation can be solved [30] at a given temperature T to obtain the AC susceptibility and thereby the SAR. Next, the latter is used in (2) to solve it for $T(t)$, which in turn is plugged into Landau-Lifshitz-Langevin equation and so on. The whole process should converge to the solution \mathfrak{S} and T . Such a numerical procedure will be followed in a future work. In the situation of interest to us here, the SAR \mathfrak{S} (or power \mathcal{P}), is obtained from an analytical expression of the AC susceptibility χ_{ac} , see [15–17]. However, the temperature enters in a rather involved way, explicitly through the coefficients of χ_{ac} and, implicitly, through the relaxation time nested in χ_{ac} . Therefore, if we consider the nonlinear corrections to χ_{ac} , as was done in Ref. [16], the differential equation (3) can only be numerically solved. In fact, in the general situation, even if only the linear contribution is used in χ_{ac} , no simple analytical expression can *a priori* be derived for the time rise of temperature $T(t)$. In this case, we may content ourselves with a numerical solution of Eq. (2) upon inserting an analytical expression for χ_{ac} given in Refs. [15–17], which we summarize now.

The SAR \mathfrak{S} of a nanomagnet, of volume V and magnetic moment $m = M_s V$, subjected to an AC magnetic field $H(t) = h \cos(\omega t)$ is given by [15, 31]

$$\mathfrak{S}(T) = \frac{\mu_0 h^2}{2} \omega \chi''(T) \quad (4)$$

where the out-of-phase component of the AC susceptibility $\chi = \chi' - i\chi''$ reads (in the Debye approximation)

$$\chi''(T) = \chi_{\text{eq}} \frac{\eta}{1 + \eta^2} \quad (5)$$

with the equilibrium susceptibility

$$\chi_{\text{eq}}(T) = \frac{\mu_0 m^2}{3k_B T}. \quad (6)$$

η is the reduced relaxation time, *i.e.*, $\eta \equiv \omega \tau_{\text{eff}}$, where τ_{eff} is the effective relaxation time given by

$$\tau_{\text{eff}}^{-1} = \tau_{\text{N}}^{-1} + \tau_{\text{B}}^{-1} \quad (7)$$

with τ_{N} being the Néel relaxation time related with the motion of the net magnetic moment in the energy potential of the NM and τ_{B} , the Brown relaxation time related with the physical motion of the NM within the fluid. More precisely, in zero DC magnetic field and using the usual notation, we have

$$\omega \tau_{\text{N}} = \frac{\sqrt{\pi} \omega \tau_0}{2 \sqrt{\sigma}} e^{\sigma}, \quad \sigma(T) = \frac{KV}{k_B T} \quad (8)$$

according to the Arrhenius law and [32]

$$\tau_B = \frac{3\xi V_H}{k_B T}$$

where ξ is the viscosity of the medium (fluid); for maghemite, $\xi = 0.00235$ kg/m/s (or 0.00235 Pa.s). V_H is the hydrodynamic volume that is larger than the magnetic volume $V = 4\pi R^3/3$ of a NM of radius R . In general, V_H is much larger than V [18, 33], since the hydrodynamic radius may be up to 50 nm more than the magnetic one.

Summarizing, we have

$$\mathfrak{S}(T) = \frac{\mu_0 h^2}{2} \omega \chi_{\text{eq}}(T) \frac{\eta(T)}{1 + \eta(T)^2}. \quad (9)$$

In order to give estimates of the various physical parameters, we have to give each term appearing in Eq. (2) a clear meaning. Accordingly, for a given magnetic substance, most often maghemite or magnetite, the power \mathcal{P} divided by the mass of the magnetic substance (m_{Fe}) yields the SAR \mathfrak{S} in W/g. Then, the constant C_{ff} in Eq. (2), which is defined by $C_{\text{ff}} = m_{\text{bf}} c_v(\text{bf}) + m_{\text{Fe}} c_v(\text{Fe})$, will be replaced by the specific heat $c_{\text{ff}} \equiv C_{\text{ff}}/m_{\text{Fe}}$ which is measured in J/K/g while $[C_{\text{ff}}] = \text{J/K}$. Likewise, we define the coefficient $l_{\text{ff}} \equiv L_{\text{ff}}/m_{\text{Fe}}$ ($[l_{\text{ff}}] = \text{W/K/g}$). Note that the specific heat c_{ff} may also be rewritten as

$$c_{\text{ff}} = c_v(\text{Fe}) + \frac{\rho_{\text{bf}}}{\rho_{\text{Fe}}} c_v(\text{bf}). \quad (10)$$

where ρ_{bf} is the density of the base fluid and ρ_{Fe} the concentration of the magnetic substance in the fluid.

C. Balance equation and temperature profile

Now, comes the discussion of the coefficient l_{ff} , which is measured in W/K/g. This should be interpreted as the analog of Newton's coefficient of heat transfer between the whole ferrofluid and its environment which may be the container or air. This is an unknown parameter that depends on the sample (its shape, size, etc), and for which it is rather difficult to come up with a simple and precise expression. So, in the present context, it is regarded as a free parameter that could be estimated from experiment. Let us, however, attempt to estimate its value and limits. At initial time, $t = 0$, or say at short times, the heat just generated by the nanomagnets diffuses through the ferrofluid, without yet reaching out to the environment. At this stage, we may set $l_{\text{ff}} = 0$ and obtain the equation

$$c_{\text{ff}} \left. \frac{dT}{dt} \right|_{t \simeq 0} = \mathfrak{S}(T). \quad (11)$$

This is the equation used in experiments [19, 20] to infer the SAR from the measurements of the initial slope of

temperature elevation. As time evolves, the heat generated and diffused within the ferrofluid starts to “trickle” into the environment. This means that the coefficient L_{ff} (or l_{ff}) acquires nonzero values, and eventually the system (ferrofluid + its environment) reaches a steady state in which the temperature of the ferrofluid is governed by Eq. (3), assuming that L_{ff} does not depend on T . As $t \rightarrow \infty$, the amount of heat generated within the ferrofluid and that lost to the environment become equal and the sample temperature remains constant at $T_{\text{max}} = T_0 + \Delta T_{\text{max}}$ with $\Delta T_{\text{max}} = \mathfrak{S}/l_{\text{ff}}$. Hence, the heat-transfer coefficient l_{ff} may be inferred from the asymptotic value of the temperature rise and the corresponding SAR observed in experiments.

Now, with the newly defined coefficients, Eq. (2) becomes

$$c_{\text{ff}} \frac{dT}{dt} = \mathfrak{S} - l_{\text{ff}} [T(t) - T_0]. \quad (12)$$

However, it is more convenient to work with a dimensionless equation. For this purpose, we introduce the time scaling factor (similar to a “relaxation time”), $\varsigma = c_{\text{ff}}/l_{\text{ff}}$ and thereby the dimensionless time $\tau \equiv t/\varsigma$. Next, we define the relative temperature rise $\theta(t) \equiv (T - T_0)/T_0$ and the dimensionless SAR $\Xi \equiv \mathfrak{S}/(T_0 l_{\text{ff}})$ so that Eq. (12) yields the final form of the equation we have to solve in order to obtain the temperature time profile

$$\frac{d\theta}{d\tau} = -\theta(\tau) + \Xi[\theta(\tau)]. \quad (13)$$

Note that for the numerical solution of this equation, the variable T in the expression of SAR given in Eq. (9) has to be replaced by $T = T_0(1 + \theta)$.

In our discussion above regarding the solution of Eq. (2), or (13), we emphasized the fact that, in the most general situation, it is not easy to obtain an analytical expression for the time profile of the temperature elevation. However, in practice we note that for maghemite, for instance, $\theta_{\text{max}} = (\Delta T)_{\text{max}}/T_0$ is about $25/318 \simeq 0.08$ and as such we may analytically solve Eq. (13) upon expanding $\Xi(\theta)$ to first order in θ . In order to illustrate this in a simple manner, we ignore the contribution of the Brownian motion to the relaxation time in Eq. (7). Doing so, we obtain the solution

$$\theta(\tau) = \frac{\Xi(T_0, h, \omega)}{\Gamma(T_0, h, \omega)} \left[1 - e^{-\Gamma(T_0, h, \omega)\tau} \right] \quad (14)$$

with $\Xi(T_0, h, \omega)$ being simply the dimensionless SAR evaluated at T_0 and

$$\Gamma(T_0, h, \omega) = 1 + \Xi(T_0, h, \omega) \Omega(T_0, \omega)$$

where

$$\Omega(T_0, \omega) = \frac{(1 + 2\sigma_0) + (3 - 2\sigma_0)\eta_0^2}{2(1 + \eta_0^2)}, \quad \sigma_0 = \frac{KV}{k_B T_0}$$

and $\eta_0 \equiv \eta(T_0)$, see Eq. (8). The temperature elevation ΔT is analytically obtained from Eq. (14) upon multiplying by T_0 . It is straightforward to extend this solution using the effective relaxation time τ_{eff} instead of τ_N .

Note that in practice, for the physical parameters of prototypical ferrofluids used in MH, the second term in $\Gamma(T_0, h, \omega)$ turns out to be a very small number. As such, $\theta(\tau) \propto (1 - e^{-\tau})$, which goes to 1 for long times leading to the saturation of ΔT observed in experiments [18, 20] and discussed above. This is indeed the profile that obtains from Eq. (3) when rewritten in the same notation as Eq. (14), namely $\theta(t) = (T - T_0)/T_0$, $\Delta T_{\text{max}}/T_0 = \theta_{\text{max}}$, and $\tau = t/\zeta$, leading to $\theta(t) = \theta_{\text{max}}(1 - e^{-\tau})$. This comparison establishes the connection between our approach and the ‘‘asymptotic’’ time behavior in Eq. (3). In particular, we see that, in a more general situation, both the rate of temperature elevation, $\Gamma(T_0, h, \omega)$, and the prefactor, $\Xi(T_0, h, \omega)/\Gamma(T_0, h, \omega)$, depend in a non trivial way on the AMF amplitude and frequency and the sample temperature.

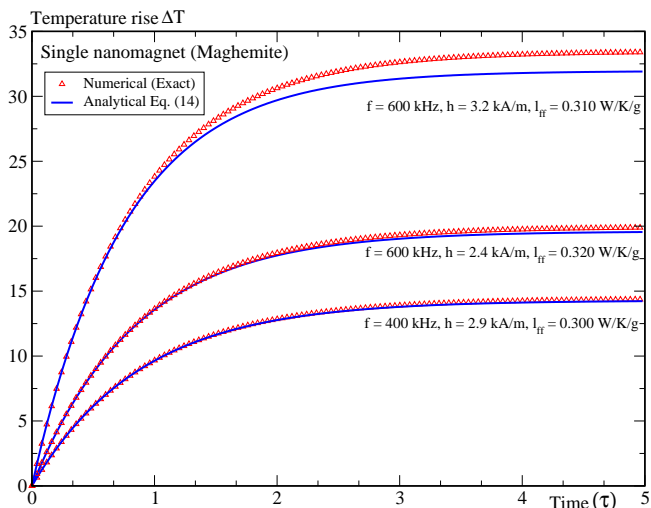


Figure 2: Time profile of the temperature elevation in a single NM: a comparison of the numerical solution of Eq. (13), in symbols, with the analytical approximation (14), in full blue lines. The physical parameters are taken from Fig. 5 for maghemite assuming a monodisperse assembly.

In Fig. 2, we compare the results from the numerical (exact) solution of Eq. (13) to the analytical approximation in Eq. (14), using the data for maghemite as in Fig. 5 and assuming a monodisperse assembly of nanomagnets with a diameter of 15.2 nm (see next Section). We see that the analytical expression in Eq. (14) is a rather good approximation for relatively low frequency and/or small amplitude of the AMF. However, the experimental data in Figs. 4 and 5 (for magnetite and maghemite) are only available up to $\tau \sim 0.6$, and in this range the analytical and the numerical solutions cannot be distinguished on the scale used for the plots in Fig 2. We could have included the curves from the asymptotic behaviour $\theta(t) = \theta_{\text{max}}(1 - e^{-\tau})$, from Eq. (3), but for this

we would need to manually insert, for each set of physical parameters, the asymptotic value θ_{max} if it is known.

We may conclude then that the analytical profile in Eq. (14) recovers very well the time profile of the temperature elevation in single nanomagnets, as obtained from the balance equation (13). This comparison is given here for the example of maghemite but should apply to any substance as long as the condition that $\Delta T/T_0$ remains small for the linear approximation underlying Eq. (14) to be valid. Obviously, the same agreement should obtain for a dilute assembly as well.

Incidentally, we already see that the increase of the AMF amplitude has a stronger effect than that of increasing its frequency [see further discussion in the next Section].

III. EFFECTS OF FIELD AMPLITUDE AND FREQUENCY: COMPARISON WITH EXPERIMENTS

We have (numerically) solved the differential equation (13) and derived the time profile of the temperature rise within the ferrofluid for both a single NM and an assembly thereof, using the effective relaxation time τ_{eff} given by Eq. (7). We have calculated the temperature profile $T(t)$ upon varying the relevant physical parameters; we have considered the two examples of maghemite and magnetite for which experimental data are available. For the assembly, we consider the case closest to the samples investigated for MH, namely polydisperse assemblies with randomly distributed anisotropy axes; the volume distribution is given by the log-normal law

$$W(V, \delta) = \frac{1}{\delta\sqrt{2\pi V}} e^{-\log^2(V/V_m)/(2\delta^2)}.$$

with the mean volume V_m and standard deviation δ . Then, the SAR of the assembly is given by the volume average (W is already normalized)

$$\overline{\mathfrak{S}}(\omega, T, h | V_m, \delta) = \int W(V, \delta) \mathfrak{S}(\omega, T, h, V) dV. \quad (15)$$

In the following sections, we will discuss our results and compare them with experiments performed on two prototypical NM assemblies most often used in MH applications, namely assemblies of maghemite and magnetite NM studied in Refs. [18] and [20], respectively. For later use, we now summarize the physical parameters for these systems.

For magnetite, we will mainly refer to and compare with the data provided by Shah et al. [20], namely nanoparticles with iron oxide concentration of $8.6\text{mg}/\text{cm}^3$ and a diameter of 9nm; an anisotropy constant $K = 3 \times 10^4\text{J}/\text{m}^3$, a saturation magnetization $M_s = 480 \times 10^3\text{A}/\text{m}$, and a density $\rho = 5.2\text{g}/\text{cm}^3$. The anisotropy field is taken equal to $0.96K/M_s$, due to the random distribution of easy axes.

Let us now discuss the specific heat and “relaxation time” defined respectively in Eqs. (10) and (13). Using the data for magnetite in water, as studied by Shah *et al.* [20], we have: $c_v(\text{bf}) = c_v(\text{water}) \simeq 4.184 \text{ J/K/g}$ and $c_v(\text{Fe}) = c_v(\text{magnetite}) \simeq 3.8 \times 10^3 \text{ J/K/L}$, or using the density of magnetite (5.2 g/cm^3), we get $c_v(\text{Fe}) \simeq 0.731 \text{ J/K/g}$. These parameters of the two ferrofluid components are independent of the sample studied in MH experiments. Now, in a given experiment one uses a specific mixture (or ferrofluid), *i.e.* with a given ratio $m_{\text{bf}}/m_{\text{Fe}}$ or $\rho_{\text{bf}}/\rho_{\text{Fe}}$. Shah *et al.* [20] used 1.2 mL of magnetite ferrofluid (magnetite in water) and a concentration $\rho_{\text{Fe}} \simeq 8.6 \text{ mg/mL} \simeq 8.6 \text{ kg/m}^3$ of magnetite in the ferrofluid. From this we infer the ferrofluid specific heat $c_v(\text{ferrofluid}) \equiv [m_{\text{bf}}c_v(\text{bf}) + m_{\text{Fe}}c_v(\text{Fe})]/m_{\text{total}} \simeq 4.156 \text{ J/K/g}$, which is slightly smaller than that of water. This is reasonable knowing that the amount of magnetic substance is very small compared to the total mass of the ferrofluid. The mass of Fe is given by $m_{\text{Fe}} = \rho_{\text{Fe}}V_{\text{ff}} \simeq 1.032 \times 10^{-2} \text{ g}$. Finally, the constant c_{ff} for the sample studied by Shah *et al.* [20] evaluates to $c_{\text{ff}} \simeq 486.43 \text{ J/K/g}$.

For maghemite, we use the data for the samples studied by Murase *et al.* [18]. These are superparamagnetic iron oxide particles (Resovist) coated with carboxy-dextran with a volume fraction of $\phi = 0.0035$ (or a concentration of 5.58 mg/cm^3) and a diameter of 15.2 nm. The magnetic characteristics of maghemite are: $K = 0.47 \times 10^4 \text{ J/m}^3$, $M_s = 414 \times 10^3 \text{ A/m}$, $\rho = 4.9 \text{ g/cm}^3$. Then, we obtain for the maghemite ferrofluid $c_{\text{ff}} \simeq 750.4 \text{ J/K/g}$.

A. Effect of AMF amplitude and frequency

In Fig.3, we plot the temperature rise as obtained from Eq. (13) using the data for magnetite ferrofluids. On the left, the results are for a varying frequency of the AMF with fixed amplitude ($h = 38.2 \text{ kA/m}$) and, on the right, for a varying amplitude and fixed frequency ($f = 194 \text{ kHz}$). Note that the highest values of the temperature elevation correspond to temperatures that exceed the water boiling point. In fact, we have extended the time range solely to see that the temperature profile formally reaches an asymptote.

These temperature profiles agree very well with those observed in experiments (see below for a quantitative comparison). We have seen that, for both maghemite and magnetite, the asymptotic values of the temperature elevation ΔT are higher for the assembly of nanoparticles than for a single particle (not shown here), but this obviously depends on D_m and δ .

For the two substances, we see that the initial slope of the temperature rise, *i.e.* $\Delta T/\Delta t|_{t=0}$, increases with the AMF frequency as was observed in experiments [18]. This stems from the fact that $\mathfrak{S} \sim \omega^2$ (for high frequencies), see Eq. (9) remembering that $\eta \sim \omega$. Similarly to the frequency effect, the maximum temperature elevation

increases with the AMF amplitude ($\mathfrak{S} \sim h^2$). The effect of the AMF amplitude is, however, stronger than that of its frequency because, in fact, the latter also appears in the denominator of \mathfrak{S} since $\mathfrak{S} \sim \omega^2/(1 + \tau_{\text{eff}}^2\omega^2)$, see Eq. (9).

B. Heat transfer coefficient

Now, we discuss the coefficient of heat transfer l_{ff} .

In the general Newton’s law of cooling at a solid-fluid interface [29], the heat flux may be related to the difference between the solid surface temperature T_s and the bulk fluid temperature T_0 : $Q = h(T_s - T_0)$ and the coefficient h depends on various parameters. For example, in the case of a fluid flowing around submerged objects, *e.g.* spheres of radius R , the coefficient h is proportional to R^2 . The study of the specific case of convective heat transfer in magnetic nanofluids, *e.g.* $\text{Fe}_2\text{O}_3/\text{water}$, is a very active research which aims at a more precise characterization of the heat transfer coefficient as a function of the applied magnetic field and the NM assembly properties [22, 23, 35]. For example, it is shown that the (convective) heat transfer coefficient is enhanced in the presence of NM and is strongly dependent on the magnetic field strength.

In analogy with Newton’s law of cooling, we have introduced the heat-transfer coefficient l_{ff} in the balance equation (2) in order to model the heat transfer at the interface between the ferrofluid and its environment. In the present study, l_{ff} is a phenomenological parameter and the approach used here to build the balance equation (2) does not allow for a derivation of the behavior of l_{ff} as a function of the system and excitation characteristics. Nevertheless, a comparison of the results rendered by this approach with the experimental data available to us today should help us infer useful hints for a more elaborate investigation of this coefficient and its characterization in MH ferrofluids.

Accordingly, in Figs 4 and 5 we plot (in full curves) the time profiles of the temperature rise obtained from Eq. (13), for varying AMF amplitude and frequency. The symbols are the experimental data reported in Refs. [20] for magnetite and in [18] for maghemite ferrofluids. Overall, we see that the time profile of temperature rise in ferrofluids, such as $\gamma\text{-Fe}_2\text{O}_3$ and Fe_3O_4 in water, is well described by the balance equation (13). This good quantitative agreement is made possible by an adjustment of the only “free” parameter provided by the (phenomenological) heat-transfer coefficient l_{ff} . This agreement is also supported by the value of the simplest coefficient of determination defined by $R^2 = 1 - \Sigma_{\text{res}}/\Sigma_{\text{tot}}$, where $\Sigma_{\text{res}} = \sum_{i=1}^{\mathcal{N}} [(\Delta T)_{\text{exp}}^i - (\Delta T)_{\text{theo}}^i]^2$ is the residual sum of squares and $\Sigma_{\text{tot}} = \sum_{i=1}^{\mathcal{N}} [(\Delta T)_{\text{exp}}^i - \overline{\Delta T}]^2$ the total sum of squares, with $\overline{\Delta T} = (1/\mathcal{N}) \sum_{i=1}^{\mathcal{N}} (\Delta T)_{\text{exp}}^i$. Indeed, for the curves in Fig. 4 (magnetite), for instance,

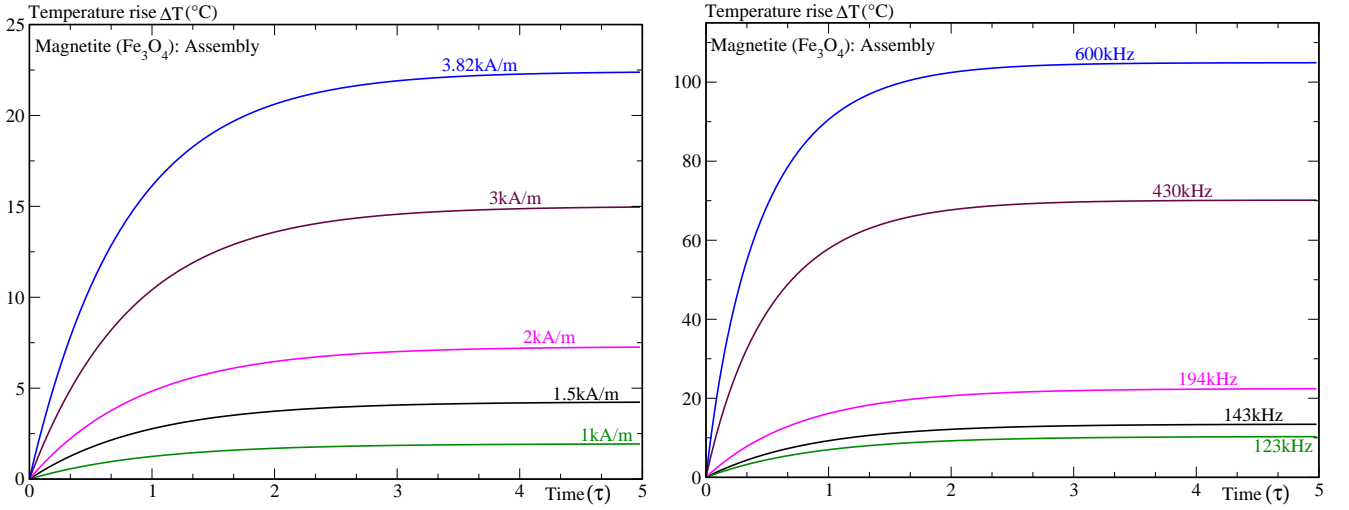


Figure 3: Time profile of temperature rise in magnetite NM with $D_m = 9$ nm, $\delta = 0.25$. (Left) varying the AMF amplitude at fixed frequency ($f = 194$ kHz) and (right) varying the AMF frequency at fixed amplitude ($h = 38.2$ kA/m).

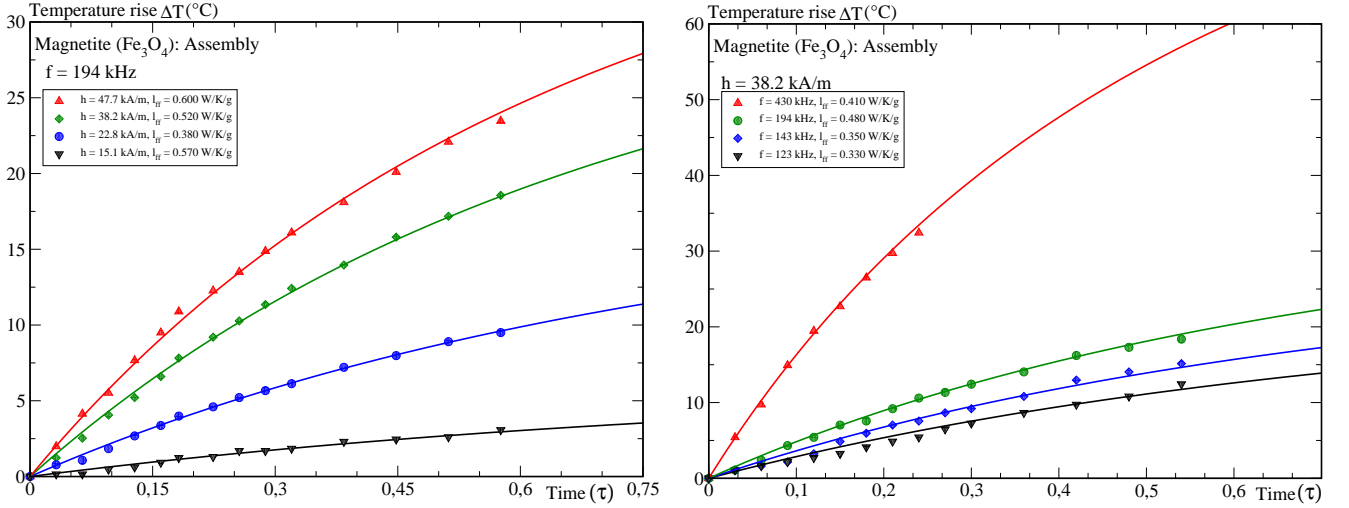


Figure 4: Time profile of the temperature rise i) in symbols, experimental data for magnetite (Figs. 4 & 5, Ref. [20]) and ii) in full lines, as obtained from Eq. (13). (Left) for different values of the AMF amplitude and $f = 194$ kHz and (right) for different values of its frequency and $h = 38.2$ kA/m. The heat transfer coefficient l_{ff} is indicated for each (best) fit.

we obtain $R^2 \sim 0.99$ for almost all curves ; we have also estimated that an uncertainty of $1K$ in the temperature elevation corresponds to $\Delta l_{ff} \simeq 10^{-2}$.

A more stringent goodness-of-fit test could be performed if more experimental data were available for the AMF amplitude and frequency and the model extended to interacting assemblies. Nevertheless, the adjustment we perform here allows us to obtain an estimate of the coefficient l_{ff} for magnetite and maghemite ferrofluids and for different values of AMF amplitude and frequency. In a more elaborate theory of heat transfer in ferrofluids and their interface with the external environment, the Newton heat-transfer coefficient should depend on the features of the system (NM+bf) as well as the external stimulus. However, in the present phenomenological

approach, the collection of data extracted from a comparison to experiments, is not sufficient for assessing the global behavior of l_{ff} . Nevertheless, this indicates the range of l_{ff} values for such system configurations and gives a first hint as how it could behave as a function of the AMF characteristics. Indeed, we mentioned earlier that l_{ff} may be inferred from experiments using the saturated temperature elevation (ΔT_{max}) and the corresponding SAR $\mathfrak{S}(T_{max})$. This implies that in this long-time regime, l_{ff} should follow the behavior of the SAR, in terms of its dependence on h, ω and the NM volume distribution (D_m, δ). In the intermediate times, usually explored in experiments and reported in Figs. 4, 5, the behavior of l_{ff} is subtler. Indeed, as far as we can tell from these data for maghemite and magnetite, l_{ff} seems

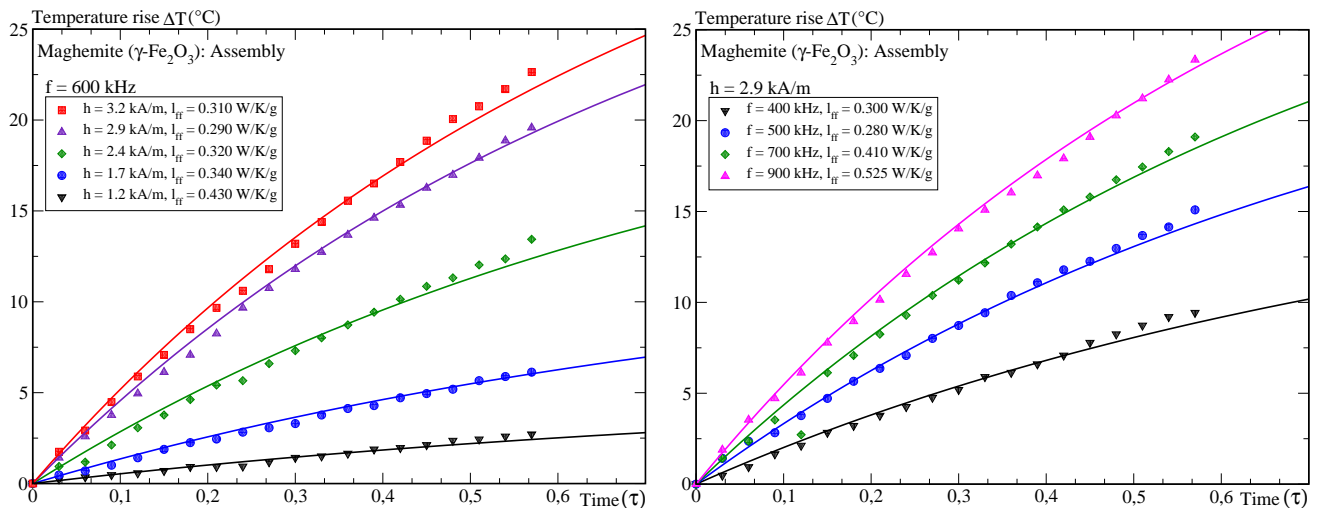


Figure 5: Time profile of the temperature rise i) in symbols, experimental data for maghemite (Figs. 7a & 8a, Ref. [18]) and ii) in full lines, as obtained from Eq. (13). (Left) for different values of the AMF amplitude and $f = 600\text{kHz}$ and (right) for different values of its frequency and $h = 2.9\text{kA/m}$. The heat transfer coefficient l_H is indicated for each (best) fit.

to be a monotonously increasing function of the AMF frequency while it exhibits a non regular variation with respect to the amplitude.

All in all, here we provide a first attempt to characterize this coefficient but further experimental and theoretical investigations are required in order to build a function for l_H in terms of the characteristics of both the AMF and the NM assembly.

IV. CONCLUSION

We have built a simple formalism for studying the heat generated by magnetic nanoparticles subjected to an alternating magnetic field and its transfer to the sample's environment, with the assumption that temperature equilibration within the ferrofluid is much faster than the heat exchange between the ferrofluid and its external environment. This formalism is based on i) the linear dynamic response of the (non-interacting) assembly of nanomagnets given by the ac susceptibility which renders the specific absorption rate of the system, and ii) a balance (phenomenological) equation that describes the heat transfer at the interface between the ferrofluid and its environment with the help of Newton's law of cooling. The latter involves a heat transfer coefficient that helps characterize the heat flow and the rate of temperature elevation within the ferrofluid. The balance equation has been numerically solved and a good approximate analytical solution has been provided.

Using our formalism, we studied the temporal profile of the temperature rise as a function of the magnetic field frequency and amplitude and have favorably compared it to the available experiments on magnetite and maghemite ferrofluids. We have thus confirmed that an increase of these parameters enhances the specific absorp-

tion rate and thereby the temperature elevation in the prototypical ferrofluids studied in experiments, namely maghemite and magnetite in water. We have also discussed the behavior of the Newton heat-transfer coefficient for these samples using the available data for various amplitudes and frequencies of the magnetic field. The data collected by fitting our theoretical results to the experimental curves provide a few hints regarding the behavior of this coefficient but are not sufficient to draw a general or universal tendency. For the latter, one should also take into account the mechanisms of heat diffusion within the nanofluid.

We suggest that this Newton's coefficient, introduced here to quantify the heat transfer from the ferrofluid to its environment, could be used as a new handle for optimizing the temperature rise in ferrofluids. Its experimental studies should provide us with valuable hints for building more refined models to better describe the mechanisms of heat generation and its diffusion in ferrofluids used in applications such as magnetic hyperthermia. In particular, its dependence on the volume fraction of nanomagnets and their mutual interactions in the ferrofluid is crucial for such applications.

Data availability

The data that support the findings of this study are available from the corresponding author upon reasonable request.

- [1] J. Overgaard, *History and heritage: an introduction*, in *Hyperthermic Oncology*, edited by J. Overgaard (Taylor and Francis, London, 1985), vol. 2, pp. 8–9.
- [2] J. Van der Zee, *Ann. Oncol.* **13**, 1173 (2002).
- [3] Johannsen M, Gneveckow U, Eckelt L, Feussner A, Waldöfner N, Scholz R, Deger S, Wust W, Loening S A and Jordan A, *Int. J. Hyperthermia* **21**, 637 (2005).
- [4] A. Skumiel, A. Jósefczak, M. Timko, P. Kopčanský, F. Herchl, M. Koneracká, and N. Tomašovičová, *Int. J. Thermodynamics* **28**, 1461 (2007).
- [5] K. Murase, H. Takata, Y. Takeuchi, and S. Saito, *Phys. Medica* **29**, 624 (2013).
- [6] C. Streffer and D. van Beuningen, *The biological basis for tumor therapy by hyperthermia and radiation*, in *Hyperthermia and the therapy of malignant tumors*, edited by C. Streffer (Springer, Berlin, 1987), pp. 24–70.
- [7] H.L. Rodríguez-Luccioni, M.M. Latorre-Estevés, J.J. Méndez-Vega, O.O. Soto, A. R. Rodríguez, C.C. Rinaldi, M.M. Torres-Lugo, *Int. J. Nanomed.* **6**, 373 (2011).
- [8] J. Carrey, B. Mehdaoui, and M. Respaud, *Journal of Applied Physics* **109**, 083921 (2011), URL <http://scitation.aip.org/content/aip/journal/jap/109/8/10.1133.1.3651582>.
- [9] B. Mehdaoui, A. Meffre, J. Carrey, S. Lachaize, L.-M. Lacroix, M. Gougeon, B. Chaudret, and M. Respaud, *Advanced Functional Materials* **21**, 4573 (2011), ISSN 1616-3028, URL <http://dx.doi.org/10.1002/adfm.201101243>.
- [10] C. Martínez-Boubeta, K. Simeonidis, A. Makridis, M. Angelakeris, O. Iglesias, P. Guardia, A. Cabot, L. Yedra, S. Estradé, F. Peiró, et al., *Scientific reports* **3**, 1652 (2013), URL <http://dx.doi.org/10.1038/srep01652>.
- [11] I. Conde-Leboran, D. Baldomir, C. Martínez-Boubeta, O. Chubykalo-Fesenko, M. P. del Morales, G. Salas, D. Cabrera, J. Camarero, F. J. Teran, and D. Serantes, *The Journal of Physical Chemistry C* **119**, 15698 (2015); S. Ruta, R. Chantrell, and O. Hovorka, *Sci Rep* **5**, 9090 (2015); D. Serantes et al., *J. Phys. Chem. C*, **118**, 5927–5934 (2014).
- [12] A. Kostopoulou and A. Lappas, *Nanotechnology Reviews* **4**, 595 (2015).
- [13] L.-M. Lacroix, R. B. Malaki, J. Carrey, S. Lachaize, M. Respaud, G. F. Goya, and B. Chaudret, *Journal of Applied Physics* **105**, 023911 (2009), URL <http://dx.doi.org/10.1063/1.3068195>.
- [14] B. Mehdaoui, J. Carrey, M. Stadler, A. Cornejo, C. Nayral, F. Delpech, B. Chaudret, and M. Respaud, *Appl. Phys. Lett.* **100**, 052403 (2012), URL <http://scitation.aip.org/content/aip/journal/apl/100/5/10.1063/1.3681361>.
- [15] J.-L. Déjardin, F. Vernay, M. Respaud, and H. Kachkachi, *Journal of Applied Physics* **121**, 203903 (2017), <https://doi.org/10.1063/1.4984013>, URL <https://doi.org/10.1063/1.4984013>.
- [16] J.-L. Déjardin, F. Vernay, and H. Kachkachi, *Journal of Applied Physics* **128**, 143901 (2020), <https://doi.org/10.1063/5.0018685>, URL <https://doi.org/10.1063/5.0018685>.
- [17] J.-L. Déjardin and F. Vernay and H. Kachkachi, *Efficiency of energy dissipation in nanomagnets: a theoretical study of ac susceptibility*, in *Magnetic Nanoparticles in Human Health and Medicine*, edited by M. Rai and C. Caizer (SPRINGER-VERLAG, 2020), vol. xxx, p. xxx.
- [18] K. Murase, J. Oonoki, H. Takata, R. Song, A. Angraini, P. Ausanai, and T. Matsushita, *Radiological Physics and Technology* **4**, 194 (2011), ISSN 1865-0341, URL <https://doi.org/10.1007/s12194-011-0123-4>.
- [19] I. Andreu and E. Natividad, *International Journal of Hyperthermia* **29**, 739 (2013), <https://doi.org/10.3109/02656736.2013.826825>, URL <https://doi.org/10.3109/02656736.2013.826825>.
- [20] R. R. Shah, T. P. Davis, A. L. Glover, D. E. Nikles, and C. S. Brazel, *Journal of Magnetism and Magnetic Materials* **387**, 96 (2015), ISSN 0304-8853, URL <http://www.sciencedirect.com/science/article/pii/S0304885315001130>.
- [21] M. Afrand, D. Toghraie, and Nima sina, *Int. Comm. Heat and Mass Transfer* **75**, 262 (2016).
- [22] E. Esmaeili, R. Gh. Chaydreh, and S. A. Rounaghi, *Appl. Thermal Eng.* **110**, 1212 (2017).
- [23] L. Sha, Y. Ju, H. Zhang, J. Wang, *Appl. Thermal Eng.* **110**, 1212 (2017).
- [24] P. Keblinski, S. R. Phillpot, S.U.S. Choi, and J.A. Eastman, *Int. J. Heat and Mass Transfer* **45**, 855 (2002).
- [25] G. Cahill, W. K. Ford, K. E. Goodson, G. D. Mahan, A. Majumdar, H. J. Maris, R. Merlin, S. R. Phillpot, *J. Appl. Physics* **93**, 793 (2003).
- [26] Y. Xuan, Q. Li, X. Zhang, and M. Fujii, *J. Appl. Physics* **100**, 855 (2006).
- [27] T. G. Desai, *J. Appl. Physics* **98**, 193107 (2011).
- [28] D. G. Cahill, P. V. Braun, G. Chen, D. R. Clarke, S. Fan, K. E. Goodson, P. Keblinski, W. P. King, G. D. Mahan, A. Majumdar, H. J. Maris, S. R. Phillpot, E. Pop, and L. Shi, *Appl. Phys. Reviews* **1**, 011305 (2014).
- [29] R. B. Bird, W. E. Stewart, E. N. Lightfoot, *Transport phenomena* (John Wiley & Sons, 2007).
- [30] Garcia-Palacios, J.L. and Lazaro, F.J., *Langevin-dynamics study of the dynamical properties of small magnetic particles*, *Phys. Rev. B* **58**, 14937 (1998).
- [31] R. Rosensweig, *Journal of Magnetism and Magnetic Materials* **252**, 370 (2002), ISSN 0304-8853, proceedings of the 9th International Conference on Magnetic Fluids, 23-27 Jul. 2001, URL <http://www.sciencedirect.com/science/article/pii/S0304885301001130>.
- [32] Yu. Raikher and M.I. Shliomis, *Adv. Chem. Phys.* **87**, 595 (1994).
- [33] G. Vallejo-Fernandez, O. Whear, A. G. Roca, S. Hussain, J. Timmis, V. Patel, and K. O’Grady, *Journal of Applied Physics* **46**, 312001 (2013), URL <https://doi.org/10.1088/0022-3727/46/31/2F312001>.
- [34] K. Murase, H. Takata, Y. Takeuchi, and S. Saito, *Physica Medica: European Journal of Medical Physics* **29**, 624 (2013), URL <http://dx.doi.org/10.1016/j.ejmp.2012.08.005>.
- [35] A. Amrollahi, A.M. Rashidi, R. Lotfi, M. Emami Meibodi, K. Kashefi, *Int. Comm. Heat and Mass Transfer* **37**, 717 (2010).